CHEMISTRY
A European Journal

A Journal of
ChemPubSoc Europe

Accepted Article

Title: Intra- vs. intermolecular hydrogen bonding: Solvent-dependent conformational preferences of a common supramolecular binding motif from 1H-NMR and VCD spectra

Authors: Daniel P. Demarque and Christian Merten

This manuscript has been accepted after peer review and appears as an Accepted Article online prior to editing, proofing, and formal publication of the final Version of Record (VoR). This work is currently citable by using the Digital Object Identifier (DOI) given below. The VoR will be published online in Early View as soon as possible and may be different to this Accepted Article as a result of editing. Readers should obtain the VoR from the journal website shown below when it is published to ensure accuracy of information. The authors are responsible for the content of this Accepted Article.

To be cited as: *Chem. Eur. J.* 10.1002/chem.201703643

Link to VoR: http://dx.doi.org/10.1002/chem.201703643

Supported by
ACES

WILEY-VCH

10.1002/chem.201703643

WILEY-VCH

Intra- vs. intermolecular hydrogen bonding: Solvent-dependent conformational preferences of a common supramolecular binding motif from ^{1}H-NMR and VCD spectra

Daniel P. Demarque[a,b], Christian Merten*[a]

Abstract: When predicting binding properties of small molecules or larger supramolecular aggregates, intra- and intermolecular hydrogen bonds are often considered the most important factor. Spectroscopic techniques such as ^{1}H-NMR spectroscopy are typically utilized to characterize such binding events, but interpretation is often qualitative and follows chemical intuition. In this study, we compare the effects of intramolecular hydrogen bonding and solvation on two chiral 2,6-pyridinediyl-dialkylamides. In comparison with ^{1}H-NMR spectroscopy, VCD spectroscopy proved to be more sensitive to conformational changes. In fact, the change of the solvent from $CDCl_3$ to DMSO-d_6 generates mirror-image VCD spectra for the same enantiomer. Here, the common sense that the sterically less hindered group is more prone to solvation proved to be wrong according predicted VCD spectra, which clearly show that both asymmetric amide hydrogens are equally likely to be solvated, but never simultaneously. The competition between intra- and intermolecular hydrogen bonding and their importance for a correct prediction of spectral properties are discussed.

Introduction

Well-engineered hydrogen bonding motifs are key structural features of many supramolecular systems like large molecular capsules[1] and foldamers[2] as well as small receptors capable of recognizing specific structural motifs. The basis for such recognition processes is often a precisely designed binding pocket with donor (D) and acceptor (A) structures placed in such a way that they fit exactly to the targeted substrates.[3] The 2,6-pyridinediyl-dialkylamide motif is a typical DAD-structure used in recognition processes. Scheme 1a shows an application of such a motif with chiral side groups, which could successfully be used in chiral recognition in HPLC to distinguish between the enantiomeric forms of the ADA-structures of glutarimides and barbiturates.[4]

[a] Daniel P. Demarque, Dr. Christian Merten
Lehrstuhl für Organische Chemie 2
Ruhr-Universität Bochum
Universitätsstraße 150
44801 Bochum, Germany
Email: christian.merten@ruhr-uni-bochum.de
Web: www.rub.de/chirality
[b] Daniel P. Demarque
Núcleo de Pesquisa em Produtos Naturais e Sintéticos
Departamento de Física e Química
Faculdade de Ciências Farmacêuticas de Ribeirão Preto
Universidade de São Paulo, Brazil

Supporting information for this article is given via a link at the end of the document.

In this contribution, we investigate the intramolecular hydrogen bonding (H-bonding) of two chiral 2,6-pyridinediyl-dialkylamides **1** and **2** (Scheme 1b), and its solvation with dimethylsulfoxide (DMSO). The initial motivation for this study was the observation that, in contrast to the chiral receptor shown in Scheme 1a, the new diamides did not show any noteworthy interactions even with achiral glutarimide (data not shown). This was evident from a lack of shifts of the NH-protons in ^{1}H-NMR spectra of mixtures (for **1**), and from the vibrational spectra of the mixtures simply being superpositions of the spectra of the components (for **2**). We attributed this behaviour to the presence of an intramolecular hydrogen bond (H-bond) between the methoxy groups and the adjacent NH-protons (as indicated in Scheme 1b),[5] which might prevent the efficient binding of the glutarimide. We thus became interested in exploring whether solvation with strongly H-bonding DMSO can break this intramolecular bond.

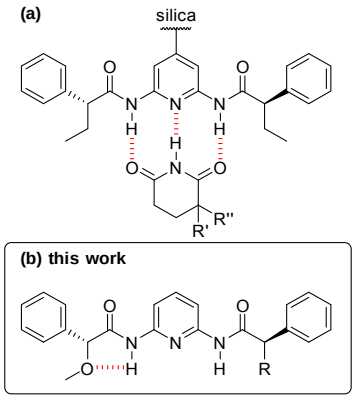

Scheme 1. (a) Application of the 2,6-pyridinediyl-dialkylamide motif in chiral recognition processes for chiral 2,2-disubstituted glutarimides and barbiturates (b) structures of the investigated compounds **1** (R=OCH_3) and **2** (R=H).

Although ^{1}H-NMR spectroscopy is commonly used to study supramolecular binding events, its relatively long timescale often makes it rather insensitive to subtle conformational changes. In contrast, as fast vibrational spectroscopic method, VCD spectroscopy has been shown to be uniquely sensitive to chirality[6] including chiral supramolecular folding[7] and other intermolecular interactions.[8] Therefore, in this study, we compare results from ^{1}H-NMR spectroscopy with infrared and vibrational circular dichroism (VCD)[9] spectroscopic information for the examples of **1** and **2** in order to investigate the role of the intramolecular H-bond in these systems. Thereby, we also compare the sensitivities for the occurring conformational

Accepted Manuscript

This article is protected by copyright. All rights reserved.

changes in solution phase and highlight important implications for VCD spectra predictions.

Results and Discussion

^{1}H-NMR spectra. The range of the aromatic and NH-protons of the ^{1}H-NMR spectra of **1** and **2** recorded in $CDCl_3$ and DMSO-d_6 are shown in Figure 1. For $CDCl_3$ solution, the ^{1}H-spectrum generally features only few signals suggesting a C_2-symmetric structure of **1** with the NH-protons at 8.94 ppm. The similarity in the chemical shift of the NH-proton of **2** (8.81 ppm; approximately 7.7 for benzyl side) indicates, that the NH-group conformation and thus also the spatial orientation of the methoxy group are similar to **1**. In DMSO-d_6, as it can nicely be observed in the range of the aromatic protons, the spectra of both compounds do not show symmetric peak pattern anymore. In case of **1**, the NH-protons are split into two very close peaks at 9.96 and 9.95 ppm, which would be consistent with the assumption that one of the NH-protons is interacting with DMSO-d_6, while the other is free respectively still in an H- bond with the methoxy group. For **2**, the formerly buried NH-proton of the benzyl substituted side is shifted into a prominent position at 10.46 ppm due to intermolecular interaction with a solvent molecule, and the other NH-proton is found at a similar chemical shift (9.68 ppm) as observed for **1**. Hence, judging by the positions of the NH-protons in DMSO-d_6, it can tentatively be assumed that the intermolecular interaction with the sulfoxide is strong enough to break the intramolecular H-bond between the methoxy group and the adjacent NH-group in **1**, while it is not clear if the bond is also broken in **2**.

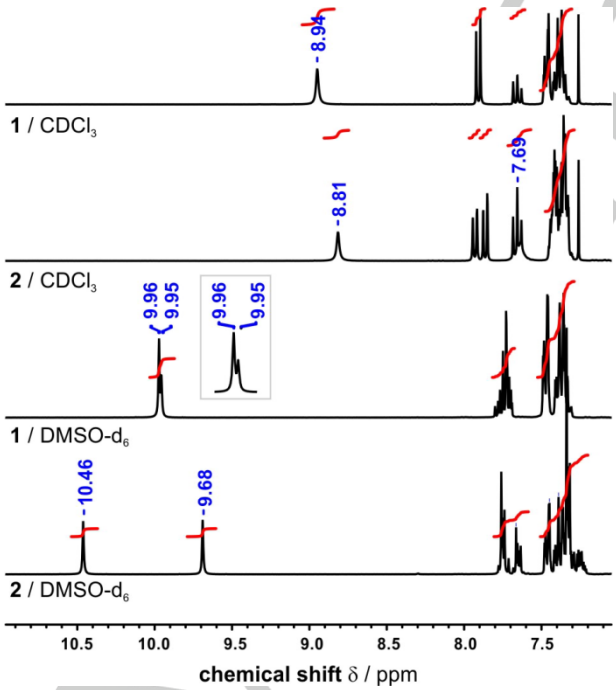

Figure 1. ^{1}H-NMR spectra of **1** and **2** in $CDCl_3$ and DMSO-d_6. The marked peaks correspond to the NH-protons.

Experimental IR and VCD spectra. In order to further investigate the conformational preferences and in particular the H-bonding interaction with DMSO, we recorded the IR and VCD spectra of *(S)*-**1** and *(S)*-**2** in both investigated solvents (Figure 2). Comparing the IR spectra, a striking overall similarity between the spectra of both compounds is noticeable, which does not allow a differentiation between the compounds. Also the direct comparison of the IR spectra taken in the two solvents does not reveal significant differences besides a decrease in intensity of the IR band about 1500 cm^{-1}. In contrast, the change of the solvent has a dramatic effect on the appearance of the VCD spectra of both *(S)*-**1** and *(S)*-**2**: Except for the prominent amide C=O stretching vibrations around 1700 cm^{-1}, the signs of all major VCD bands changed. This observation not only shows that a simple solvent change can make the VCD spectrum of a molecule look partially like the opposite enantiomer, it also suggests a major structural change.

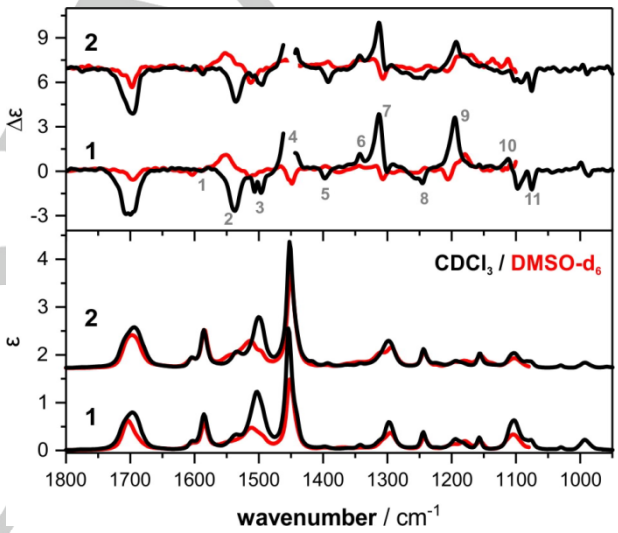

Figure 2. Experimental VCD and IR spectra of **1** and **2** in $CDCl_3$ and DMSO-d_6 recorded at 0.1 M concentration and 100 µm path length. The band numbering is identical for both sets of spectra. The gaps in VCD bands 4 are due to a too strong absorbance of the parent IR band.

A qualitative approach to the interpretation of the similarity between the VCD spectra of *(S)*-**1** and *(S)*-**2** may lead to the conclusion that both compounds would behave essentially the same in solution. This would suggest a coordination of DMSO to the NH-proton of the common structural motif of both compounds, namely the α-methoxyphenyl propionic (αMPP-)amide. Intuitively, however, the coordination of DMSO to the benzylic amide of **2** would be expected to be more favorable due to steric reasons as well as due to the proposed intramolecular H-bond between the methoxy and NH group. In order to shed further light on these somewhat contradicting qualitative explanations of the H-bonding, we carried out spectra calculations.

Conformational analysis. The theoretical analysis of the IR and VCD spectra of **1** and **2** first requires a comprehensive

Accepted Manuscript

This article is protected by copyright. All rights reserved.

10.1002/chem.201703643

conformational analysis of the two compounds. Therefore, the following rotations around several torsional angles were evaluated: the orientation of the amide group expressed as the angles $\alpha_{1,2}$ spanning N_{ar}-C_{ar}-N_H-$C_{(=O)}$, the spatial orientation of the phenyl ring with respect to the amide group as $\beta_{1,2}$ over N_H-$C_{(=O)}$-C^{α}-C_{ar}, and the conformation of the methoxy group as $\gamma_{1,2}$ via $C_{(=O)}$-C^{α}-O-C (see SI for more details). The conformers generated by systematic variation of these angles were subjected to geometry optimizations at the B3LYP/6-311+G(2d,p)/IEFPCM($CHCl_3$) level of theory. Similar to the findings for the closely related pyridine-2,6-dicaboxamides,[10] the cis-conformation of the amide group places the carbonyl group in close vicinity to the lone pair of the pyridine-nitrogen, which leads to a significant repulsion and thus to a higher energy for all cis-conformations. Accordingly, the lowest energy conformations of both **1** and **2** are found to exclusively adopt trans-conformations of the amide groups. The characteristic geometric parameters $\beta_{1,2}$ and $\gamma_{1,2}$ of the two molecules are summarized in Tables 1 and 2 together with the relative energies and Boltzmann populations. In addition, full details on all optimized conformations can be found in the supporting information file (Tables S1 and S2).

Table 1. Summary of the most important lowest energy conformations of *(S)*-**1**, which all feature a trans-conformation for both α_1 and α_2, including the number of intramolecular MeO··H-N H-bonds in the conformation (#hb), the relative Gibbs free energy at 298K (ΔG, in kcal/mol) and the corresponding Boltzmann population (p, in percentage), and the angles $\beta_{1,2}$ and $\gamma_{1,2}$ (in degree).

1-[a]	#hb	ΔG[b]	p	β_1	β_2	γ_1	γ_2
c1tt	2	0.00	77.4	117.0	117.0	-163.3	-163.3
c1gt	2	0.82	19.3	97.0	118.4	-81.3	-162.6
c1gg	2	1.97	2.8	97.1	97.3	-81.0	-81.4
c2gt	1	3.51	0.2	-86.9	118.2	-69.7	-163.0
c2tt	1	3.77	0.1	-94.0	116.8	-168.9	-163.1
c2gg	1	4.78	0.0	-89.2	97.4	-69.2	-81.5
c2tg	1	5.20	0.0	-91.6	97.8	-168.7	-81.9
c3gt	0	7.46	0.0	-86.6	-88.4	-69.9	-168.9
c3gg	0	7.12	0.0	-85.6	-85.6	-69.9	-69.9
c3tt	0	8.46	0.0	-94.5	-94.5	-168.6	-168.6

[a] conformer-id cX_{gt}: X represents the combination of β_1 and β_2, and the subscripts *g* and *t* refer to γ_1 and γ_2

[b] Referenced to G = -1355.530071 hartree of **1**-$c1_{tt}$

For the symmetrically substituted **1**, the conformations featuring two intramolecular H-bonds are clearly favored, and the symmetric conformation **1**-$c1_{tt}$ (cf. Figure 3) is the most dominant conformer. While the rotation of the methoxy groups into a gauche-(-)-conformation already slightly increases the conformational energies (0.8 kcal/mol, **1**-c1tt → **1**-c1gt), breaking the H-bonds is in both cases connected to large costs in energy (3.5 kcal/mol, **1**-c1tt → **1**-c2tt). The conformational analysis thus confirms the interpretation of the ^{1}H-NMR spectra of **1** in $CDCl_3$, which suggested a symmetric conformation.

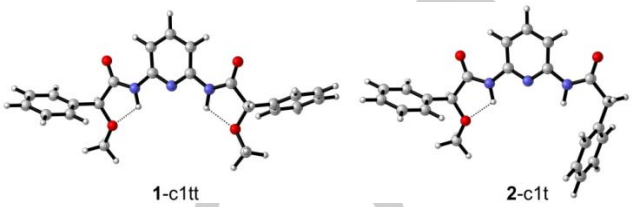

Figure 3. Lowest energy conformers of *(S)*-**1** and *(S)*-**2** in $CDCl_3$.

Table 2. Summary of the most important lowest energy conformations of *(S)*-**2**, which all feature a trans-conformation for both α_1 and α_2, including the number of intramolecular MeO··H-N H-bonds in the conformation (#hb), the relative Gibbs free energy at 298K (ΔG, in kcal/mol) and the corresponding Boltzmann population (p, in percentage), and the angles $\beta_{1,2}$ and γ_1 (in degree).

2-[a]	#hb	ΔG[b]	p	β_1	β_2	γ_1
c1t	1	0.00	61.4	117.8	-0.2	-162.5
c1g	1	1.26	7.3	97.1	1.0	-81.2
c2g	1	2.06	1.9	96.8	99.1	-81.1
c2t	1	1.36	6.2	118.2	103.5	-162.7
c3g	1	2.32	1.2	97.7	-97.2	-81.7
c3t	1	1.39	5.9	119.3	-87.0	-162.7
c4g	1	0.87	14.0	97.0	165.7	-81.4
c4t	1	2.27	1.3	118.3	178.0	-162.9
c5g	0	3.03	0.4	-88.2	-4.5	-96.0
c5t	0	3.69	0.1	-92.0	-4.0	-139.0
c6g	0	4.51	0.0	-87.3	-85.5	-95.8
c6t	0	5.35	0.0	-91.6	-95.9	-139.0
c7g	0	4.55	0.0	-87.9	-178.0	-95.9
c7t	0	5.31	0.0	-93.3	177.8	-138.9
c8g	0	5.05	0.0	-86.2	103.2	-95.5
c8t	0	5.17	0.0	-96.3	96.6	-138.8

[a] conformer-id cX_{gt}: X represents the combination of β_1 and β_2, and the subscripts *g* and *t* refer to γ_1

[b] Referenced to G = -1241.005623 hartree of **2**-$c1_g$

The benzylic amide in asymmetric *(S)*-**2** is found to feature a larger conformational flexibility than the αMPP-amide side, as the angle β_2 can adopt four different orientations instead of two: gauche-(-) and trans as for **1**, as well as gauche-(+) and also syn ($\beta_2 \approx 0$). While showing the expected stabilizing MeO··H-N H-bonds, the two most populated conformations of **2** are in fact

Accepted Manuscript

This article is protected by copyright. All rights reserved.

those in which β_2 is in the syn conformation (cf. Figure 3). The rotation of the benzyl group into the g+ or g- conformation is predicted to increase the energy already by 1.3 kcal/mol (**2**-c1t → **2**-c2t or c3t), comparable to rotation of the methoxy group (1.2 kcal/mol, **2**-c1t → **2**-c1g). As observed already for **1**, the breaking of the intramolecular H-bond requires more energy than the aforementioned conformational changes (3 kcal/mol, **2**-c1t → **2**-c5t). In further support of this conformational preference, it should be noted that the syn-conformation of the benzyl group is in agreement with the chemical shift of the NH proton at 7.7 ppm, which indicates a strong shielding due to the location above the phenyl ring.

Based on the optimized geometries of **1**-c1 and **1**-c2, we followed a micro-solvation approach[8e, 11] and generated mono-solvated structures by placing one molecule DMSO-d_6 near each of the NH-groups. Consequently, we obtained two solvated structures for each conformer (except for the C_2-symmetric conformers **1**-c1tt and **1**-c1gg, which yielded only one structure as both NH-groups are identical), i.e. 12 solvated conformers in total. This solvation-step had an interesting effect on the conformational equilibrium (Table S3): It shifted towards the **1**-c2 conformer family, with the DMSO bound to the NH group, which is not in an intramolecular H-bond (cf. Figure 4). The coordination of DMSO to the amide proton thus provides enough stabilizing energy to cleave the intramolecular H-bond, which consequently leads to a conformational change of the αMPP-amide group. A weak interaction between the α-CH further stabilizes the solvated complex and, based on the single point energies of each of the components (**1**-c2gt, **1**-c2gt··DMSO, and DMSO), leads to a total stabilization by 4.3 kcal/mol. Taking into account also the conformational change from the lowest energy structure **1**-c1tt to **1**-c2gt, the binding of DMSO results in a stabilization by 1.9 kcal/mol. Based on the conformational distribution of **1**··DMSO, the tentative analysis of ^{1}H-NMR spectrum of **1** (see above) can thus be confirmed.

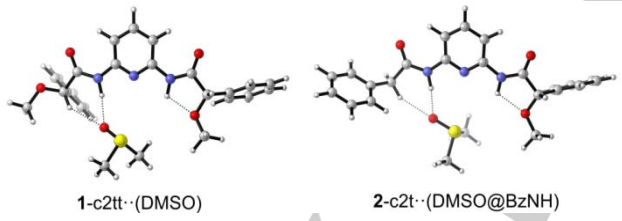

Figure 4. Lowest energy conformers of mono-solvated *(S)*-**1** and *(S)*-**2** in DMSO-d_6.

Following the same procedure, the asymmetric substitution in **2** leads to a large number of conformers as, in addition to the two non-equal NH-groups, also the higher conformational flexibility of the benzylic amide has to be considered. The 16 conformers listed in Table 2 would thus lead to 32 solvated conformers. The syn-conformation of the benzylic amide, however, is often not possible due to sterical hindrance with DMSO. Moreover, the trans-conformation of the torsional angle β_2 is also not found as stable structure, as the α-protons of the benzyl group also weakly interact with DMSO and thus pull the benzyl group into g+ or g- orientations. Consequently, the actual number of conformers is strongly reduced to 17.

Consistent with the large ^{1}H-NMR shift of the benzylic amide NH proton, the predicted relative energies of the solvated conformers reveals a clear preference for the solvation of the benzylic amide proton (cf. Table S4) and shows that it is energetically significantly favored over the cleavage of the intramolecular H-bond. The most populated conformer **2**-c2t··(DMSO@BzNH), which is shown in Figure 4, contributions with 72 % to the overall Boltzmann population; overall, the group of DMSO@BzNH conformers account for >99 %. Similar to the conformer solvation energy of **1**-c2tg discussed above, the interaction energy accounts for 4.1 kcal/mol with respect to the non-solvated conformer **2**-c2t. However, when compared to the non-solvated lowest energy structure **2**-c1t though, solvation of the amide group with DMSO releases 3.6 kcal/mol, i.e. about twice as much energy as for **1**. In agreement with the observations for **1**, the solvation of the αMPP-amide group in **2** also generally stabilizes conformers without intramolecular H-bond. Within the group of DMSO@αMPP-NH conformers, **2**-c8t is the lowest energy structure, which is stabilized by 1.0 kcal/mol with respect to the non-solvated structure **2**-c1t.

Analysis of the IR/VCD spectra. For the analysis of the vibrational spectra, single-conformer IR and VCD spectra were predicted for all optimized conformers and averaged according to their respective Boltzmann weights (Tab. 1, 2, S1-S4). For each of the investigated molecules, we thus obtained two sets of spectra: one for isolated (non-solvated) form and one for DMSO-solvated form.

Figure 5 shows a comparison of simulated spectra with the experimental ones of *(S)*-**1** (superpositions provided in Figure S1) In the top panel, the agreement between the experimental spectra for $CDCl_3$ solution and the predicted spectra for the isolated form can be seen to be very good. In both the IR and VCD spectrum, the band assignments indicate that all major bands are well reproduced. Solely the calculated intensity of the amide stretching vibration at 1700 cm^{-1} appears to be too high, which is mainly related to the broader line width in the experiment compared to the uniformly broadened theoretical spectra. Similarly, the experimental spectra for **1** in DMSO-d_6 are reproduced exceptionally well by the simulation of the solute-solvent complex. As again indicated by the band assignments, the IR and VCD absorbance patterns are exactly reproduced and no VCD band seems to be predicted with the wrong sign. Therefore, the analysis of the vibrational spectra of **1** confirms the predicted conformational preferences (Table 1 and S1).

Accepted Manuscript

This article is protected by copyright. All rights reserved.

10.1002/chem.201703643

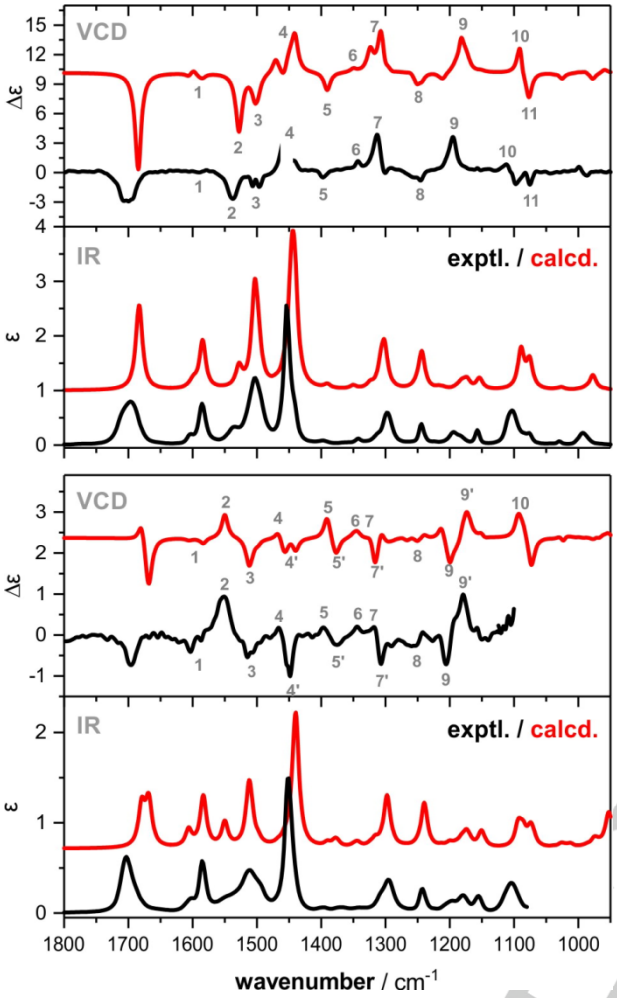

Figure 5. Experimental VCD and IR spectra of *(S)*-**1** in CDCl3 (top) and DMSO-d_6 (bottom) recorded at 0.1 M (100 µm pathlength) in comparison to the calculated spectra of *(S)*-**1** and the mono-solvated complex *(S)*-**1**··DMSO. The intensities of the calculated spectra of the solvated complex in the bottom panel are scaled by a factor of 0.5. The numbers indicate band assignment of the most important spectral features.

During the detailed analysis of the spectra, an observation was made, which is worth noting from a spectroscopic perspective. When the entries for the **1**-c1 conformers in Table 1 are neglected, the conformer **1**-c2gt becomes the new the lowest energy structure. After adjusting the Boltzmann populations, the IR and VCD spectra simulated based on this new conformational distribution are found to be almost identical with those calculated for **1**··DMSO (cf. Figure S2). In other words, the coordination of DMSO to **1** does not cause significant spectral changes to each single conformer spectrum, but solely alters the conformer energies.

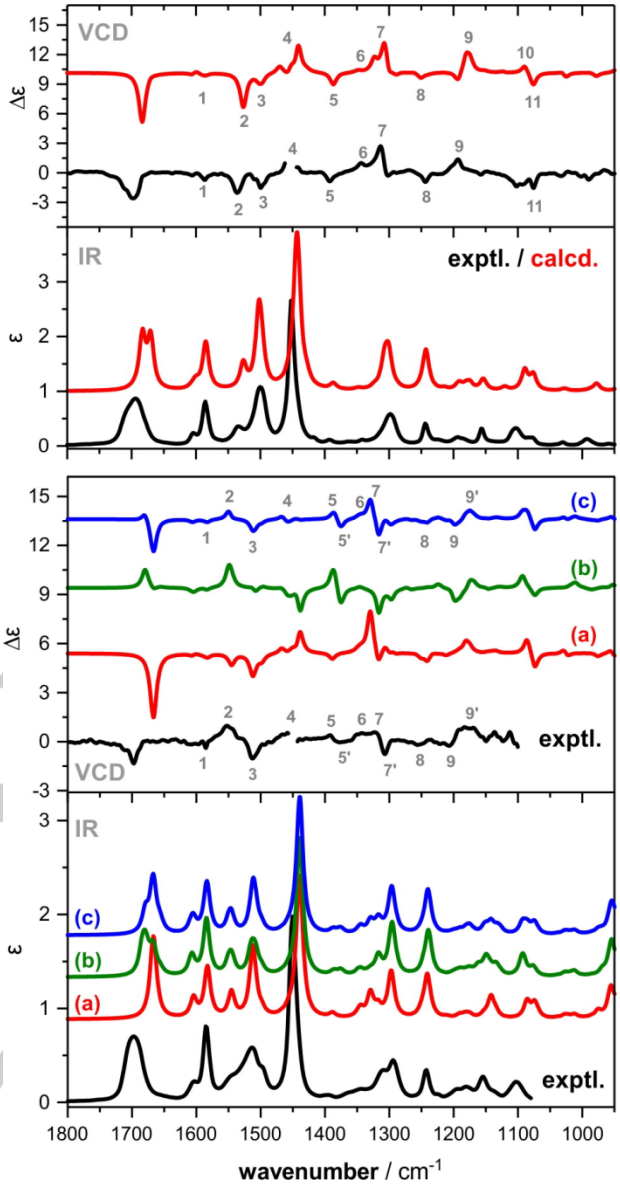

Figure 6. Experimental VCD and IR spectra of *(S)*-**2** in CDCl3 (top) and DMSO-d_6 (bottom) recorded at 0.1 M (100 µm pathlength) in comparison to calculated spectra. Top panel: Calculated spectra of non-solvated *(S)*-**2**; bottom panel: mono-solvated complex *(S)*-**2**··DMSO based on (a) all conformers, (b) only DMSO@αMPP-NH conformers, and (c) a 1:1 mixture of the two sets of spectra. The intensities of the calculated spectra of the solvated complex are scaled by a factor of 0.5. The numbers indicate band assignment of the most important spectral features.

Continuing with the spectra analysis of *(S)*-2, an equally good agreement between the predicted spectra for the non-solvated molecule with the experimental data recorded in $CDCl_3$ solution can be notice (Figure 6, top). All major bands are reproduced, although few bands, like band 10, are slightly obscured due to baseline imperfections. Nevertheless, the spectra clearly support the above presented conformational analysis.

Accepted Manuscript

This article is protected by copyright. All rights reserved.

Unlike in the case of **1**, the predicted IR and VCD spectra for mono-solvated **2** do not fully agree with the experimental spectra (Figure 6, bottom, traces a). In fact, a significant number of bands are predicted incorrectly. For instance, band 2 features a strong positive band in the experiment, but the calculation predicts a negative signal at the same frequency. Furthermore, bands 5/5' are observed as (+/-)-signal, but theoretically predicted to be one solely negative feature. Likewise, the range around bands 6 and 7 shows a very intense band in the predicted spectrum, but two weak positive signals in the experiment. In the IR spectrum, mainly the range from 1350-1300 cm^{-1} does not fit well.

The changes in the spectra of **1** were nicely explained by a cleavage of the intramolecular H-bond. Therefore, we also calculated IR and VCD spectra of **2** solely based on the group of DMSO@αMPP-NH conformers (Figure 6, bottom, traces b). While this only led to small changes in the simulated IR spectrum, many bands in the VCD spectrum changed: The aforementioned bands 2 and 5/5' feature the correct sign, while the sign of the C=O stretching vibration at ~1700 cm^{-1} has flipped. Accordingly, this spectrum shows a certain improvement over the simulation, which considers all conformers, but does not fully agree either.

A convincing agreement with the experimental spectra can actually be achieved when both sets of spectra are averaged, i.e. if a composite spectrum with equal contributions of DMSO@BzNH and DMSO@αMPP-NH is generated (Figure 6, bottom panel, traces c). As the band assignments indicate, such a manually weighted spectrum reproduces all bands observable in the experimental VCD spectrum. Minor discrepancies such as the residual small positive component in the VCD band of the C=O stretching band (1700 cm^{-1}) can again be neglected, as the experimental line width of the carbonyl band is larger than the simulated line broadening. Further confirmation that the composite spectrum actually provides an accurate picture of the conformational distribution can be achieved by comparing the vibrational dissymmetry factors (VDF).[12] This VDF has been introduced by Polavarapu in analogy to the *g*-factor in CD spectroscopy, and shown to be a good measure for the comparison of experimental and theoretical spectra.[13] Details on this comparison are provided in the supporting information (Figure S3).

Further structure optimizations showed that **2** could generally also bind two DMSO molecules simultaneously. For steric reasons, however, this is only possible for those conformers, in which the intramolecular hydrogen bond is broken. While this twofold solvation leads to a further stabilization in terms of calculated energies, the resulting VCD spectra actually do not agree as well as the composite spectrum in Figure 6 (cf. Figure S4 and S5). This is mainly due to some additional bands, which do not have any experimental counterparts. Therefore, in conclusion of the conformational analysis of **2** in DMSO-d_6, it can be stated that both NH of **2** are equally likely to be solvated, and that the spectra are best explained assuming an equal mixture of **2**··(DMSO@BzNH) and **2**··(DMSO@αMPP-NH) to be present. A simultaneous two-fold solvation can be excluded.

Finally, in an attempt to also interpret the ^{1}H-NMR spectra based on the experimentally confirmed conformational distributions of **1** and **2** in the two investigated solvents, we carried out proton chemical shift calculations. In comparison with the experimental data recorded in chloroform-d_1, the predictions for the NH-protons were in very good agreement, thus giving confidence in the overall conformational and ^{1}H-NMR spectral analysis. However, for both compounds, the effect of hydrogen bonding with DMSO-d_6 was systematically overestimated, which resulted in a stronger deshielding influence of the solvent molecule and therefore a larger chemical shift of the respective interacting NH-proton (cf. supporting information for further information on the ^{1}H-NMR calculations). Hence, in the present study, VCD spectroscopy provides the most decisive information on the conformational preferences of **1** and **2**, while the ^{1}H-NMR spectra, even when combined with chemical shift calculations, are significantly less conclusive.

Conclusions

In this study, we investigated two 2,6-pyridinediyl-dialkylamides **1** and **2**, which feature a common donor-acceptor-donor motif for hydrogen bonding. For the same enantiomer, the change of the solvent from $CDCl_3$ to DMSO-d_6 resulted in almost mirror-images VCD spectra. A theoretical conformational analysis predicts **1** to be in a symmetric conformation in $CDCl_3$, and one intramolecular hydrogen bond is cleaved upon solvation with DMSO-d_6. These predictions are proven to be correct on the basis of the ^{1}H-NMR and IR/VCD spectroscopic analysis. In the case of **2** in $CDCl_3$, in agreement with the theoretical predictions, the α-methoxy group is also in an intramolecular hydrogen bond and the benzylic amide adopts a syn-conformation. In DMSO-d_6, calculations suggest a preferential solvation of the benzylic amide proton. This qualitatively supports the interpretation of the ^{1}H-NMR spectrum. However, this energies-based analysis does not agree with the predicted VCD spectra, which clearly show that both amide hydrogens are equally likely to be solvated, but never solvated simultaneously.

Hence, in conclusion, this study not only underlines the importance of the intramolecular H-bonds, but also shows that a slight overestimation of the stabilization energy can lead to a wrong prediction of binding properties. Moreover, on basis of the simple examples of **1** and **2**, it can be expected that substrate binding to DAD or similar structural motifs is actually more dynamic and flexible than the ^{1}H-NMR spectra of the H-bonded complexes might suggest. Therefore, we are currently investigating further systems, which actually bind the targeted substrates, in order to further explore the binding dynamics.

Experimental Section

General. All chemicals were purchased from commercial sources (Sigma Aldrich, Germany, or Alfa Aesar, Germany) at highest available purity and used without further purification. The identities of the prepared compounds were confirmed by ^{1}H-/^{13}C-NMR spectroscopy and mass spectrometry.

Accepted Manuscript

This article is protected by copyright. All rights reserved.

Synthesis of (S,S)-1. 3.7 mmol (0.5 g) of enantiopure 2-methoxy-2-phenylacetic acid was added to 10 ml of dichloromethane (DCM) and cooled to 0ºC. To the solution was added 1-hydroxybenzotriazole (HOBt; 0.2g, 1.5 mmol) and N-(3-dimethylaminopropyl)-N'-ethylcarbonate (EDC*HCl; 0.57g, 3 mmol), and it was stirred for 30 min. After this period, 2,6-diaminopyridine (0.13g, 1.2 mmol) was added and kept stirring overnight at room temperature. The solution was partitioned with water, dried over $MgSO_4$ and purified by column chromatography using DCM:EtOAc (8:2) to yield a white solid (0.18g, 37%). NMR: ^{1}H ($CDCl_3$, 200 MHz): δ = 3.34 (s, 6H), 4.65 (s, 2H), 7.24-7.37 (m, 10H), 7.53 (t, 1H), 7.81 (d, J 8Hz, 2H), 8.87 (s, 2H). ^{13}C (CDCl3, 50 MHz): δ = 57.4, 83.9, 109.9, 127.1, 128.8, 136.4, 140.8, 149.1, 169.1.

Synthesis of (S)-2. 36.7 mmol (2.5 g) of 2-phenylacetic acid was added to 25 ml of dichloromethane (DCM) and cooled to 0ºC. To the solution was added HOBt (0.5 eq, 1.25 g, 18 mmol) and EDC*HCl (4.2g, 22 mmol), and it was stirred for 30 min. Then, 2,6-diaminopyridine (0.13g, 1.2 mmol) was added and kept stirring overnight at room temperature. The solution was partitioned with water, dried over MgSO4 and purified in chromatography column using DCM:ethyl acetate (8:2) to yield N-(6-aminopyridin-2-yl)-2-phenylacetamide 3 as a yellow oil (3.1 g, 59.4%). NMR: ^{1}H ($CDCl_3$, 200 MHz): δ = 3.34 (s, 2H), 4.29 (s, 2H), 6.90 (d, J 8 Hz, 1H), 7.14-7.24 (m, 5H), 7.30 (t, 1H), 7.43 (d, J 7.8 Hz), 7.88 (s, 1H). ^{13}C (CDCl3, 50 MHz): δ = 44.8, 103.2, 104.4, 127.5, 129.1, 129.5, 134.3, 140.1, 149.7, 157.1, 169.4. Afterwards, enantiopure 2-methoxy-2-phenylacetic acid (1.2 mmol, 0.2 g) was coupled to 3 using a similar procedure yielding colorless oil (0.433 g, 64%). NMR: 1H ($CDCl_3$, 200 MHz): δ = 3.45 (s, 3H), 3.78 (s, 2H), 4.75 (s, 1H), 7.35-7.49 (m, 10H), 7.69 (t, 1H), 7.90 (d, J 7.8 Hz, 1H), 7.96 (d, J 7.8 Hz, 1H), 8.85 (s, 1H). 13C (CDCl3, 50 MHz): δ = 45.0, 57.4, 83.8, 109.7, 127.0, 127.7, 129.3, 129.5, 128.7, 133.9, 136.3, 148.8, 149.9.

IR/VCD spectroscopy. The vibrational spectra were recorded on a Bruker Vertex 70 equipped with a PMA 50 unit for polarization modulated measurements. Solutions of the samples were held in a transmission cell with BaF_2 windows with 100µm path length. Both IR and VCD spectra were recorded at 4 cm^{-1} spectral resolution by accumulating 32 respectively ~20000 scans (4 hrs accumulation time). Baseline correction of the VCD spectra was done by subtraction of the spectra of the racemic mixture recorded under identical conditions. The spectra are presented in molar absorptivity ε (in 10^3 M^{-1} cm^{-1}) and differential molar absorptivity $\Delta\varepsilon$ (in 10^{-2} M^{-1} cm^{-1}). Due to strong solvent absorbance, the investigated spectral ranges for $CDCl_3$ and DMSO-d_6 are 1800-950 cm^{-1} and 1800-1100 cm^{-1}.

Computational details. Geometry optimizations and frequency calculations were performed for *(S)*-**1** and *(S)*-**2** at the B3LYP/6-311+G(2d,p) basis set using the Gaussian 09 E.01 software package with tight convergence criteria and ultrafine integration grids.[14] Solvent effects were taken into account either implicitly by using the integral equation formalism of the polarizable continuum model (IEFPCM),[15] or explicitly by placing DMSO-d_6 molecules at certain binding positions (see text). Vibrational line broadening was simulated by assigning a Lorentzian band shape with half-width at half-height of 6 cm^{-1} to the calculated dipole and rotational strength. Finally, the calculated wavenumbers were scaled by a factor of 0.98. NMR shielding tensors were calculated using the Gauge-Independent Atomic Orbital (GIAO) method.[16]

The energy gain due to H-bonding to DMSO-d_6 was estimated as $\Delta E_{hb} = E_{(conf\cdot\cdot DMSO)} - E_{conf} - E_{DMSO}$, with the electronic energies of the optimized solute-solvent complex ($E_{(conf\cdot\cdot DMSO)}$), the same conformer without solvent molecule attached (E_{conf}), and DMSO-d_6 (E_{DMSO}). Herein, the reference structure E_{conf} is either the conformer, to which the DMSO was bound, or the lowest energy conformer. This then leads to the energy gain solely due to the H-bonding, or under simultaneous consideration of the accompanying conformational change.

Acknowledgements

CM is gratefully acknowledges financial support by the Fonds der chemischen Industrie through a Liebig fellowship, and to the Deutsche Forschungsgemeinschaft for support through the Cluster of Excellence RESOLV ("Ruhr Explores SOLVation", EXC 1069). DPD thanks FAPESP for the doctoral scholarship (2014/18052-0), and RESOLV for support of his research stay in Bochum.

Keywords: hydrogen bonding • chirality • supramolecular recognition • intermolecular interactions • vibrational circular dichroism

[1] a) O. Dumele, B. Schreib, U. Warzok, N. Trapp, C. A. Schalley, F. Diederich, *Angew. Chem. Int. Ed.* **2017**, *56*, 1152-1157; b) L. Catti, Q. Zhang, K. Tiefenbacher, *Chem. Eur. J.* **2016**, *22*, 9060–9066; c) K.-D. Zhang, D. Ajami, J. Rebek, *J. Am. Chem. Soc.* **2013**, *135*, 18064-18066

[2] D.-W. Zhang, X. Zhao, J.-L. Hou, Z.-T. Li, *Chem. Rev.* **2012**, *112*, 5271-5316.

[3] a) B. Ośmiałowski, E. Kolehmainen, R. Gawinecki, R. Dobosz, R. Kauppinen, *J. Phys. Chem. A* **2010**, *114*, 12881-12887; b) F. H. Beijer, R. P. Sijbesma, J. A. J. M. Vekemans, E. W. Meijer, H. Kooijman, A. L. Spek, *J. Org. Chem.* **1996**, *61*, 6371-6380.

[4] B. Feibush, A. Figueroa, R. Charles, K. D. Onan, P. Feibush, B. L. Karger, *J. Am. Chem. Soc.* **1986**, *108*, 3310-3318.

[5] a) J. F. Galan, J. Brown, J. L. Wildin, Z. Liu, D. Liu, G. Moyna, V. Pophristic, *J. Phys. Chem. B* **2009**, *113*, 12809-12815; b) Z. Liu, R. C. Remsing, D. Liu, G. Moyna, V. Pophristic, *J. Phys. Chem. B* **2009**, *113*, 7041-7044.

[6] a) J. Costante, L. Hecht, P. L. Polavarapu, A. Collet, L. D. Barron, *Angew. Chem. Int. Ed.* **1997**, *36*, 885-887; b) J. M. Batista Jr, E. W. Blanch, V. d. S. Bolzani, *Nat. Prod. Rep.* **2015**, *32*, 1280-1302; c) T. Bruhn, G. Pescitelli, F. Witterauf, J. Ahrens, M. Funk, B. Wolfram, H. Schneider, U. Radius, M. Bröring, *Eur. J. Org. Chem.* **2016**, *2016*, 4236-4243; d) T. Bruhn, G. Pescitelli, S. Jurinovich, A. Schaumlöffel, F. Witterauf, J. Ahrens, M. Bröring, G. Bringmann, *Angew. Chem. Int. Ed.* **2014**, *53*, 14592-14595.

[7] a) S. R. Domingos, S. J. Roeters, S. Amirjalayer, Z. Yu, S. Hecht, S. Woutersen, *Phys. Chem. Chem. Phys.* **2013**, *15*, 17263-17267; b) T. Buffeteau, L. Ducasse, L. Poniman, N. Delsuc, I. Huc, *Chem Commun* **2006**, 10.1039/b604462j, 2714-2716.

[8] a) M. Losada, P. Nguyen, Y. Xu, *J. Phys. Chem. A* **2008**, *112*, 5621-5627; b) E. Debie, L. Jaspers, P. Bultinck, W. Herrebout, B. V. D. Veken, *Chem. Phys. Lett.* **2008**, *450*, 426-430; c) M. Urbanova, *Chirality* **2009**, *21 Suppl 1*, E215-230; d) K. Bünnemann, C. Merten, *Phys. Chem. Chem. Phys.* **2017**, *19*, 18948-18956; e) C. Merten, *Phys. Chem. Chem. Phys.* **2017**, *19*, 18803-18812; f) K. Bünnemann, C. Merten, *J. Phys. Chem. B* **2016**, *120*, 9434-9442; g) C. Merten, C. H. Pollok, S. Liao, B. List, *Angew. Chem. Int. Ed.* **2015**, *54*, 8841-8845.

[9] L. A. Nafie, *Vibrational Optical Actvity*, John Wiley & Sons Ltd, UK, **2011**.

[10] J. F. Malone, C. M. Murray, G. M. Dolan, R. Docherty, A. J. Lavery, *Chemistry of Materials* **1997**, *9*, 2983-2989.

[11] M. R. Poopari, Z. Dezhahang, Y. Xu, *Phys. Chem. Chem. Phys.* **2013**, *15*, 1655-1665.

[12] a) C. L. Covington, P. L. Polavarapu, *Phys. Chem. Chem. Phys.* **2016**, *18*, 13912-13917; b) P. L. Polavarapu, C. L. Covington, *Chirality* **2014**, *26*, 539–552; c) C. L. Covington, P. L. Polavarapu, *J. Phys. Chem. A* **2013**, *117*, 3377-3386.

[13] F. M. S. Junior, C. L. Covington, A. C. F. de Albuquerque, J. F. R. Lobo, R. M. Borges, M. B. de Amorim, P. L. Polavarapu, *J. Nat. Prod.* **2015**, *78*, 2617-2623.

[14] *Gaussian 09, Rev E.01*, M. J. Frisch, G. W. Trucks, H. B. Schlegel, G. E. Scuseria, M. A. Robb, J. R. Cheeseman, G. Scalmani, V. Barone, B. Mennucci, G. A. Petersson, H. Nakatsuji, M. Caricato, X. Li, H. P. Hratchian, A. F. Izmaylov, J. Bloino, G. Zheng, J. L. Sonnenberg, M.

Accepted Manuscript

This article is protected by copyright. All rights reserved.

Hada, M. Ehara, K. Toyota, R. Fukuda, J. Hasegawa, M. Ishida, T. Nakajima, Y. Honda, O. Kitao, H. Nakai, T. Vreven, J. J. A. Montgomery, J. E. Peralta, F. Ogliaro, M. Bearpark, J. J. Heyd, E. Brothers, K. N. Kudin, V. N. Staroverov, T. Keith, R. Kobayashi, J. Normand, K. Raghavachari, A. Rendell, J. C. Burant, S. S. Iyengar, J. Tomasi, M. Cossi, N. Rega, J. M. Millam, M. Klene, J. E. Knox, J. B. Cross, V. Bakken, C. Adamo, J. Jaramillo, R. Gomperts, R. E. Stratmann, O. Yazyev, A. J. Austin, R. Cammi, C. Pomelli, J. W. Ochterski, R. L. Martin, K. Morokuma, V. G. Zakrzewski, G. A. Voth, P. Salvador, J. J. Dannenberg, S. Dapprich, A. D. Daniels, O. Farkas, J. B. Foresman, J. V. Ortiz, J. Cioslowski, D. J. Fox, Wallingford CT, USA, **2013**

[15] J. Tomasi, B. Mennucci, R. Cammi, *Chem. Rev.* **2005**, *105*, 2999-3094.

[16] J. R. Cheeseman, G. W. Trucks, T. A. Keith, M. J. Frisch, *J. Chem. Phys.* **1996**, *104*, 5497-5509.

WILEY-VCH
Accepted Manuscript

This article is protected by copyright. All rights reserved.

10.1002/chem.201703643

WILEY-VCH

Entry for the Table of Contents (Please choose one layout)

FULL PAPER

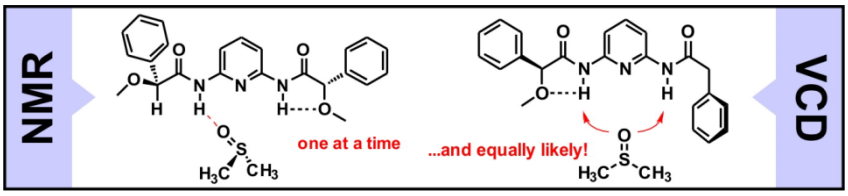

We show that the intuitive assumption of the sterically less hindered amide group being solvated preferentially does not hold for the cases of two 2,6-pyridinediyl-dialkylamides. Using VCD spectroscopy, we show that solvation in fact induces significant conformational changes which are not immediately apparent from ^{1}H-NMR data.

*Daniel P. Demarque, Christian Merten **

Page No. – Page No.

Intra- vs. intermolecular hydrogen bonding: Solvent-dependent conformational preferences of a common supramolecular binding motif from ^{1}H-NMR and VCD spectra

WILEY-VCH
Accepted Manuscript

This article is protected by copyright. All rights reserved.